The vascular endothelial growth factor inhibitor soluble FLT-1 ameliorates atopic dermatitis in APOC1 transgenic mice

Aanhold, C.C.L. van; Bus, P.; Zandbergen, M.; Bos, M.; Berbee, J.F.P.; Quint, K.D.; ... ; Baelde, H.J.

[1]*Laboratory of Human Molecular Genetics, Department of Genetics, Federal University of Paraná, Universidade Federal do Paraná, Curitiba, Paraná, Brazil*
[*]*Corresponding author e-mail: angelicaboldt@gmail.com*

SUPPLEMENTARY MATERIAL

Supplementary material is linked to the online version of the paper at www.jidonline.org, and at https://doi.org/10.1016/j.jid.2019.07.691.

REFERENCES

Batista IAA, Helguero LA. Biological processes and signal transduction pathways regulated by the protein methyltransferase SETD7 and their significance in cancer. Signal Transduct Target Ther 2018;3:19.

Bumiller-Bini V, Cipolla GA, de Almeida RC, Petzl-Erler ML, Augusto DG, Boldt ABW. Sparking fire under the skin? Answers from the association of complement genes with pemphigus foliaceus. Front Immunol 2018;9:695.

Ea CK, Baltimore D. Regulation of NF-kappaB activity through lysine monomethylation of p65. Proc Natl Acad Sci U S A 2009;106:18972–7.

Gregory BL, Cheung VG. Natural variation in the histone demethylase, KDM4C, influences expression levels of specific genes including those that affect cell growth. Genome Res 2014;24:52–63.

Hung KH, Woo YH, Lin IY, Liu CH, Wang LC, Chen HY, et al. The KDM4A/KDM4C/NF-κB and WDR5 epigenetic cascade regulates the activation of B cells. Nucleic Acids Res 2018;46:5547–60.

Lee J, Park B, Kim G, Kim K, Pak J, Kim K, et al. Arhgef16, a novel Elmo1 binding partner, promotes clearance of apoptotic cells via RhoG-dependent Rac1 activation. Biochim Biophys Acta 2014;1843:2438–47.

Liu C, Zhang F, Li T, Lu M, Wang L, Yue W, et al. MirSNP, a database of polymorphisms altering miRNA target sites, identifies miRNA-related SNPs in GWAS SNPs and eQTLs. BMC Genomics 2012;13:661.

Malheiros D, Petzl-Erler ML. Individual and epistatic effects of genetic polymorphisms of B-cell co-stimulatory molecules on susceptibility to pemphigus foliaceus. Genes Immun 2009;10:547–58.

Manczinger M, Kemény L. Novel factors in the pathogenesis of psoriasis and potential drug candidates are found with systems biology approach. PLOS ONE 2013;8:e80751.

Nisihara RM, de Bem RS, Hausberger R, Roxo VS, Pavoni DP, Petzl-Erler ML, et al. Prevalence of autoantibodies in patients with endemic pemphigus foliaceus (fogo selvagem). Arch Dermatol Res 2003;295:133–7.

Oliveira LA, Marquart-Filho A, Trevilato G, Timoteo RP, Mukai M, Roselino AM, et al. Anti-desmoglein 1 and 3 autoantibody levels in endemic pemphigus foliaceus and pemphigus vulgaris from Brazil. Clin Lab 2016;62:1209–16.

Spindler V, Drenckhahn D, Zillikens D, Waschke J. Pemphigus IgG causes skin splitting in the presence of both desmoglein 1 and desmoglein 3. Am J Pathol 2007;171:906–16.

Thaler F, Mercurio C. Compounds and methods for inhibiting histone demethylases: a patent evaluation of US20160102096A1. Expert Opin Ther Pat 2016;26:1367–70.

Westaway SM, Preston AGS, Barker MD, Brown F, Brown JA, Campbell M, et al. Cell penetrant inhibitors of the KDM4 and KDM5 families of histone lysine demethylases. 1. 3-Amino-4-pyridine carboxylate derivatives. J Med Chem 2016;59:1357–69.

Zhao M, Huang W, Zhang Q, Gao F, Wang L, Zhang G, et al. Aberrant epigenetic modifications in peripheral blood mononuclear cells from patients with pemphigus vulgaris. Br J Dermatol 2012a;167:523–31.

Zhao M, Liang G, Wu X, Wang S, Zhang P, Su Y, et al. Abnormal epigenetic modifications in peripheral blood mononuclear cells from patients with alopecia areata. Br J Dermatol 2012b;166:226–73.

The Vascular Endothelial Growth Factor Inhibitor Soluble FLT-1 Ameliorates Atopic Dermatitis in *APOC1* Transgenic Mice

Journal of Investigative Dermatology (2020) **140,** 491–494; doi:10.1016/j.jid.2019.07.700

TO THE EDITOR

Atopic dermatitis (AD) is an inflammatory skin condition characterized by scaling, lichenification, excoriations, and pruritus. Vascular endothelial growth factor (VEGF) has previously been underscored as a contributor to skin inflammation in AD (Varricchi et al., 2015). This is supported by the evidence that (1) VEGF causes hyperpermeability of vessels (Ferrara et al., 2003) leading to edema and spongiosis, (2) VEGF induces chemotaxis of myeloid cells expressing VEGF receptor 1 (e.g., macrophages, mast cells) (Sawano et al., 2001), and (3) VEGF activates endothelial cells, leading to increased expression of adhesion molecules in these cells (Kim et al., 2001), thereby promoting tissue infiltration of leukocytes. Moreover, VEGF levels are increased in skin lesions and plasma of patients with AD (Varricchi et al., 2015). Thus, VEGF-inhibiting therapy may be a promising treatment for AD.

Soluble VEGF receptor 1 or soluble fms-like tyrosine kinase-1 (sFLT-1) is a natural inhibitor of VEGF-A by acting as a decoy receptor (Shibuya, 2015). Treatment with low doses of sFLT-1 reduces inflammation and disease severity in preclinical models of several inflammatory diseases. In this study, we investigated the anti-inflammatory effects of sFLT-1 on AD in a mouse model. *APOC1* transgenic (*APOC1*-tg) mice develop AD because of a disruption of the skin lipid barrier (Nagelkerken et al., 2008) and a triggered immune system (Bus et al., 2017a). While manifesting many AD hallmarks, the *APOC1*-tg model does not fully replicate human disease. In this study, we transfected *APOC1*-tg mice with *sFlt-1* (Supplementary Figure S1). Detailed information on materials and methods used is described in Supplementary Materials. All work was approved by the Animal Experiments Committee (DEC license 13163).

Consistent with a previous report (Nagelkerken et al., 2008), *APOC1*-tg mice, and not age-matched wild-type (WT) mice, spontaneously developed

Abbreviations: AD, atopic dermatitis; APOC1, apolipoprotein C1; APOC1*-tg,* APOC1 *transgenic; sFLT-1, soluble fms-like tyrosine kinase-1; VEGF, vascular endothelial growth factor; WT, wild-type*

Accepted manuscript published online 16 August 2019; corrected proof published online 28 October 2019

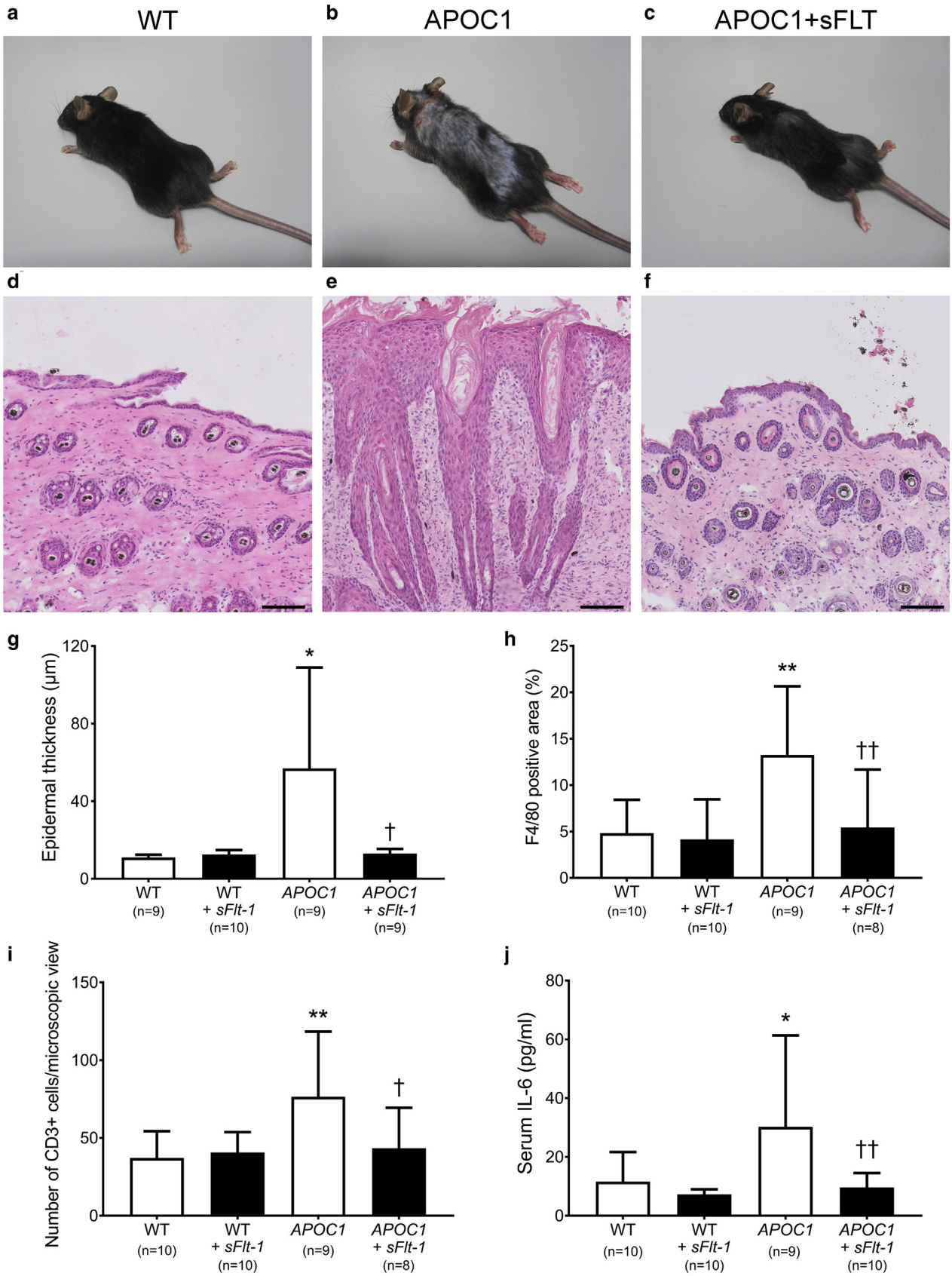

Figure 1. Transfecting *APOC1*-tg mice with *sFlt-1* ameliorates AD. (**a**–**c**) At 8 weeks of age, WT and *APOC1*-tg mice were transfected with *sFlt-1;* representative images of (a) WT, (b) *APOC1*-tg, and (c) *sFlt-1*–transfected *APOC1*-tg mice at 7 weeks after transfection. (**d**–**f**) Representative sections of the skin of (d) WT, (e) *APOC1*-tg, and (f) *sFlt-1*–transfected *APOC1*-tg mice at 15 weeks after transfection; these sections were stained with hematoxylin and eosin; the sections in (d) and (f) show a normal unaffected epidermal layer, and the section in (e) shows epidermal changes consistent with AD (spongiosis, serum crust,

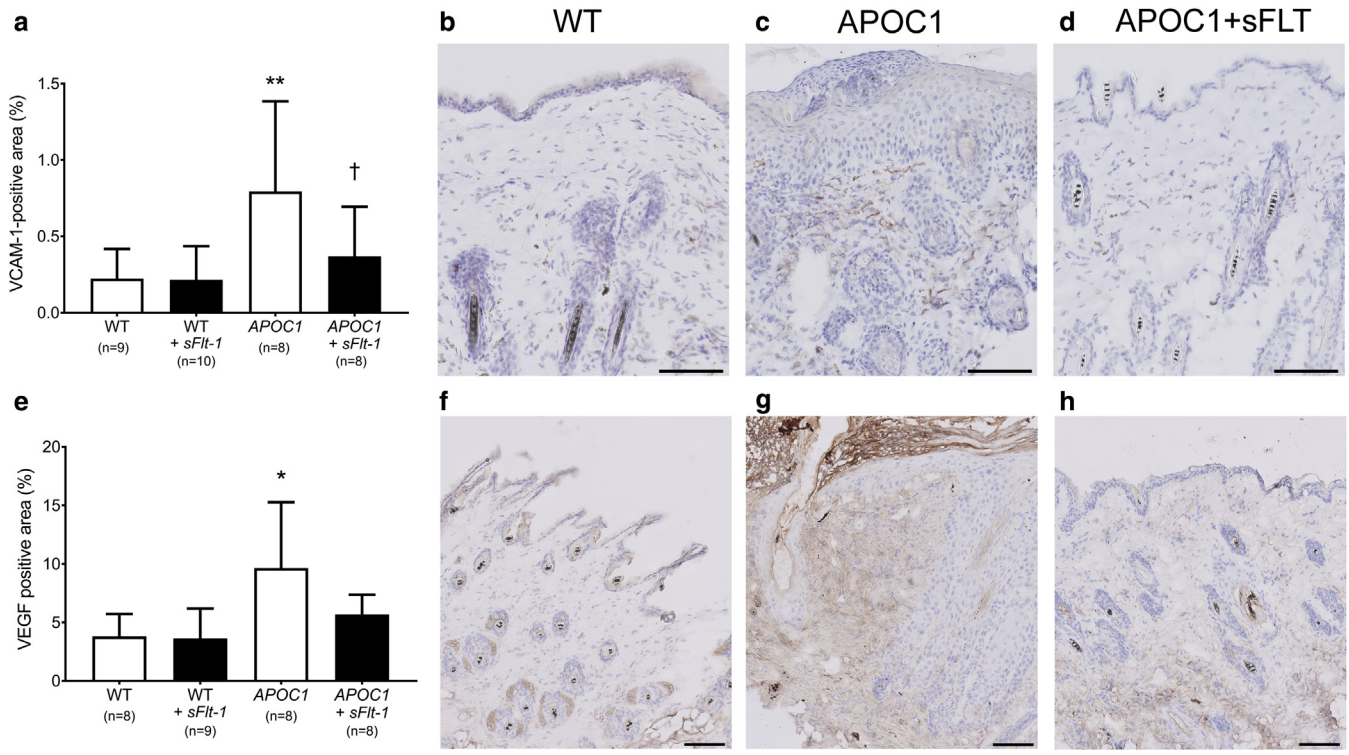

Figure 2. *sFlt-1* transfection reduces VEGF-increased VCAM-1 in the skin of *APOC1*-tg mice. (**a**) Skin VCAM-1 and (**e**) VEGF protein expression were quantified at 15 weeks after transfection in the indicated groups. (**b**–**h**) Representative images of (b–d) VCAM-1 and (f–h) VEGF immunohistochemical staining in skin sections from WT, *APOC1*-tg, and *sFlt-1*–transfected *APOC1*-tg mice at 15 weeks after transfection. Summary data are presented as the mean ± standard deviation. $*P < 0.05$ and $**P < 0.01$ versus nontransfected WT; $\dagger P < 0.05$ versus nontransfected *APOC1*-tg mice (one-way analysis of variance). APOC1, apolipoprotein C1; *APOC1*-tg, *APOC1* transgenic; *sFlt-1*, soluble fms-like tyrosine kinase-1; VEGF, vascular endothelial growth factor; WT, wild-type. Bars = 100 μm.

AD from 6 weeks of age onward (Figure 1). Transfection of 8-week-old *APOC1*-tg mice with *sFlt-1* completely resolved skin lesions, and hair growth recurred (Figure 1c and f). Quantification of the thickness of the epidermal layer at 15 weeks after transfection showed that sFLT-1 normalized epidermal thickening in *APOC1*-tg mice (Figure 1g). Furthermore, F4/80-positive areas and numbers of $CD3^+$ cells were increased in the skin of nontransfected *APOC1*-tg mice and were reduced to levels observed in WT in *sFlt-1*–transfected *APOC1*-tg mice (Figure 1h and i, and Supplementary Figure S2). Neutrophil infiltrates were also present in the skin of *APOC1*-tg mice (Supplementary Figure S2g) but were not observed in transfected mice (Supplementary Figure S2h). We next determined whether sFLT-1 reduces serum levels of proinflammatory cytokines in *APOC1*-tg mice. No differences were observed in tumor necrosis factor–α levels among groups in sera collected at 15 weeks after transfection. Nonetheless, *APOC1*-tg mice had markedly increased serum IL-6 levels compared with those of WT mice, which were normalized after transfection with *sFlt-1* (Figure 1j). Thus, sFLT-1 reduces skin lesions and inflammation in *APOC1*-tg mice.

Because we previously demonstrated that sFLT-1 decreases VEGF-induced endothelial cell activation (Bus et al., 2017b), we next determined whether sFLT-1 reduces skin inflammation in *APOC1*-tg mice by decreasing expression of the adhesion molecule, VCAM-1. Compared with WT mice, VCAM-1 was markedly increased in endothelial cells in the skin of *APOC1*-tg mice (Figure 2a and Supplementary Figure S3). Transfection with *sFlt-1* reduced VCAM-1 expression to WT (Figure 2c and d). In line with this, VEGF expression was increased in the skin of *APOC1*-tg mice compared with that of WT mice (Figure 2e). This suggests that sFLT-1 reduces VEGF-increased endothelial activation in the skin of *APOC1*-tg mice by sequestering increased VEGF levels. Other functions of sFLT-1 besides sequestering VEGF have been described; sFLT-1 plays an essential role in podocyte cell morphology and glomerular barrier function—independent of VEGF—by binding directly to the glycosphingolipid monosialodihexosylganglioside (GM3) in lipid rafts on the surface of the podocytes (Jin et al., 2012). Monocytes also express GM3, and this expression is increased upon

hyperkeratosis, acanthosis). (**g**–**j**) Summary of (g) epidermal thickness, (h) F4/80 expression in the skin, (i) number of $CD3^+$ cells in the skin, and (j) serum IL-6 levels, measured at 15 weeks after transfection in the indicated groups. Summary data are presented as the mean ± standard deviation. $*P < 0.05$ and $**P < 0.01$ versus nontransfected WT; $\dagger P < 0.05$ and $\dagger\dagger P < 0.01$ versus nontransfected *APOC1*-tg mice (one-way analysis of variance). AD, atopic dermatitis; APOC1, apolipoprotein C1; *APOC1*-tg, *APOC1* transgenic; *sFlt-1*, soluble fms-like tyrosine kinase-1; WT, wild-type. Bars = 100 μm.

differentiation of monocytes into macrophages and during inflammatory responses (Gracheva et al., 2007; Puryear et al., 2012). Therefore, sFLT-1 may bind to monocytes or macrophages via glycosphingolipid monosialodihexosylganglioside, subsequently altering cellular function. This notion is supported by the finding that sFLT-1 downregulates the FLT-1 receptor in leukocytes by decreasing the activity of the FLT-1 promoter, thereby preventing subsequent migration of these cells upon stimulation with VEGF (Krysiak et al., 2005). Thus, the anti-inflammatory effects of sFLT-1 on AD in *APOC1*-tg mice may be explained by VEGF sequestration and by a VEGF-independent mechanism.

Treatment with VEGF inhibitors has been widely associated with nephrotoxicity (Estrada et al., 2019). We previously found that *sFlt-1* transfection reversed kidney inflammation and damage in diabetic mice (Bus et al., 2017b). In line with this, this study found that *APOC1*-tg mice transfected with *sFlt-1* do not develop renal dysfunction or histological changes in the kidney (Supplementary Figure S4), although *APOC1*-tg mice are prone to develop kidney disease at a later age (Bus et al., 2017a). In contrast, sFLT-1 reduced glomerular inflammation in *APOC1*-tg mice; however, this did not reach significance within the studied time frame (Supplementary Figure S4). This suggests that sFLT-1 does not lead to kidney dysfunction and exerts its anti-inflammatory effects systemically. sFLT-1 may be a safe and promising treatment for several inflammatory diseases.

In summary, we show that sFLT-1 ameliorates skin lesions and inflammation in an AD mouse model. In *APOC1*-tg mice transfected with *sFlt-1*, thickening of the epidermis and inflammatory infiltrates in the skin remitted, along with normalization of serum levels of IL-6 and skin expression of VCAM-1, without developing renal problems during the studied period. Thus, this study shows that sFLT-1 may be a valuable treatment for patients with AD.

Data availability statement

Datasets related to this article can be found at https://doi.org/10.17632/3rrcdhcmgr.2, hosted at Mendeley (Van Aanhold, 2019).

ORCIDs

Cleo C.L. van Aanhold: http://orcid.org/0000-0001-7760-7781
Pascal Bus: http://orcid.org/0000-0001-9833-2887
Malu Zandbergen: http://orcid.org/0000-0003-3671-4059
Manon Bos: http://orcid.org/0000-0002-8636-888X
Jimmy F.P. Berbée: http://orcid.org/0000-0001-9133-3297
Koen D. Quint: http://orcid.org/0000-0002-3267-5630
Jan A. Bruijn: http://orcid.org/0000-0001-7592-250X
Hans J. Baelde: http://orcid.org/0000-0002-1214-500X

CONFLICT OF INTEREST

The authors state no conflicts of interest.

AUTHOR CONTRIBUTIONS

Conceptualization: PB, HJB; Investigation: CCLvA, PB, MZ; Resources: JFPB; Supervision: HJB; Visualization: CCLvA; Writing - Original Draft Preparation: CCLvA; Writing - Review and Editing: CCLvA, PB, MZ, JFPB, MB, KDQ, JAB, HJB.

Cleo C.L. van Aanhold[1,*], Pascal Bus[1], Malu Zandbergen[1], Manon Bos[1], Jimmy F.P. Berbée[2,3], Koen D. Quint[4], Jan A. Bruijn[1] and Hans J. Baelde[1]

[1]Department of Pathology, Leiden University Medical Center, Leiden, The Netherlands; [2]Department of Endocrinology, Leiden University Medical Center, Leiden, The Netherlands; [3]Einthoven Laboratory for Experimental Vascular Medicine, Leiden University Medical Center, Leiden, The Netherlands; and [4]Department of Dermatology, Leiden University Medical Center, Leiden, The Netherlands
[*]Corresponding author e-mail: c.c.l.van_aanhold@lumc.nl

SUPPLEMENTARY MATERIAL

Supplementary material is linked to the online version of the paper at www.jidonline.org, and at https://doi.org/10.1016/j.jid.2019.07.700.

REFERENCES

Bus P, Pierneef L, Bor R, Wolterbeek R, van Es LA, Rensen PC, et al. Apolipoprotein C-I plays a role in the pathogenesis of glomerulosclerosis. J Pathol 2017a;241:589–99.

Bus P, Scharpfenecker M, Van Der Wilk P, Wolterbeek R, Bruijn JA, Baelde HJ. The VEGF-A inhibitor sFLT-1 improves renal function by reducing endothelial activation and inflammation in a mouse model of type 1 diabetes. Diabetologia 2017b;60:1813–21.

Estrada CC, Maldonado A, Mallipattu SK. Therapeutic inhibition of VEGF signaling and associated nephrotoxicities. J Am Soc Nephrol 2019;30:187–200.

Ferrara N, Gerber HP, LeCouter J. The biology of VEGF and its receptors. Nat Med 2003;9:669–76.

Gracheva EV, Samovilova NN, Golovanova NK, Andreeva ER, Andrianova IV, Tararak EM, et al. Activation of ganglioside GM3 biosynthesis in human monocyte/macrophages during culturing in vitro. Biochemistry (Mosc) 2007;72:772–7.

Jin J, Sison K, Li C, Tian R, Wnuk M, Sung HK, et al. Soluble FLT1 binds lipid microdomains in podocytes to control cell morphology and glomerular barrier function. Cell 2012;151:384–99.

Kim I, Moon SO, Kim SH, Kim HJ, Koh YS, Koh GY. Vascular endothelial growth factor expression of intercellular adhesion molecule 1 (ICAM-1), vascular cell adhesion molecule 1 (VCAM-1), and E-selectin through nuclear factor-kappa B activation in endothelial cells. J Biol Chem 2001;276:7614–20.

Krysiak O, Bretschneider A, Zhong E, Webb J, Hopp H, Verlohren S, et al. Soluble vascular endothelial growth factor receptor-1 (sFLT-1) mediates downregulation of FLT-1 and prevents activated neutrophils from women with pre-eclampsia from additional migration by VEGF. Circ Res 2005;97:1253–61.

Nagelkerken L, Verzaal P, Lagerweij T, Persoon-Deen C, Berbee JF, Prens EP, et al. Development of atopic dermatitis in mice transgenic for human apolipoprotein C1. J Invest Dermatol 2008;128:1165–72.

Puryear WB, Yu X, Ramirez NP, Reinhard BM, Gummuluru S. HIV-1 incorporation of host-cell-derived glycosphingolipid GM3 allows for capture by mature dendritic cells. Proc Natl Acad Sci USA 2012;109:7475–80.

Sawano A, Iwai S, Sakurai Y, Ito M, Shitara K, Nakahata T, et al. Flt-1, vascular endothelial growth factor receptor 1, is a novel cell surface marker for the lineage of monocyte-macrophages in humans. Blood 2001;97:785–91.

Shibuya M. VEGF-VEGFR system as a target for suppressing inflammation and other diseases. Endocr Metab Immune Disord Drug Targets 2015;15:135–44.

Van Aanhold CCL. Dataset sFLT-1 ameliorates AD in *APOC1*-tg mice. Mendeley 2019.

Varricchi G, Granata F, Loffredo S, Genovese A, Marone G. Angiogenesis and lymphangiogenesis in inflammatory skin disorders. J Am Acad Dermatol 2015;73:144–53.

SUPPLEMENTARY MATERIALS AND METHODS

sFlt-1 transfection

Two pcDNA3.1 vectors (Invitrogen, Breda, The Netherlands) containing either *sFlt-1-VSV* or the luciferase gene were generated as described previously (Bus et al., 2017b; Eefting et al., 2007). The resulting plasmids were amplified in DH5α *E. coli* (Invitrogen), purified using the QIAfilter Plasmid Maxi-prep kit (Qiagen, Venlo, the Netherlands) and dissolved in Endo-Free Tris−EDTA buffer (Qiagen). Mice were transfected by electroporation of the *sFlt-1-VSV* and luciferase constructs into both gastrocnemius muscles (20 μg each) as described previously (Eefting et al., 2007). To monitor transfection efficiency, the mice were injected intraperitoneally with luciferin at 2-week intervals. Five minutes after each luciferin injection, luciferase activity was visualized at the transfection sites using a Night-OWL bioluminescence camera (Xenogen Ivis Spectrum, Alameda, CA) as described previously (Eefting et al., 2007). A radiance above 1×10^6 p/sec/cm^2/sr was considered as a successful transfection.

Animals

For this study, we used 8-week-old C57BL/6J mice (n = 9 males, n = 11 females; Harlan Laboratories, Indianapolis, IN) and age-matched *APOC1*-tg mice (n = 9 males, n = 11 females). All experiments were conducted in accordance with national guidelines for the care and use of experimental animals (DEC license 13163). Mice were housed in individually ventilated cages in groups of up to five mice per cage, with food and water provided ad libitum. For the experiments, mice were randomly assigned to groups: *sFlt-1*-transfected and nontransfected *APOC1*-tg mice (n = 10 per group) and *sFlt-1*−transfected and nontransfected C57BL/6J (WT) mice (n = 10 per group). At 8 weeks of age, the mice were transfected with *sFlt-1*. Fifteen weeks after transfection, the mice were killed, skin and renal tissue were collected for histological analysis, and sera were collected for cytokine quantification; this time point was chosen because we previously found that treatment with sFLT-1 for 15 weeks resulted in marked changes in kidney inflammation and histology in diabetic mice (Bus et al., 2017b). One mouse in the nontransfected *APOC1*-tg group was removed from the study because the development of severe AD complicated by open wounds. Missing samples or samples with poor tissue quality for immunohistochemistry were excluded from analysis.

Immunohistochemistry

The skin and kidney tissues were cut at 4-μm thickness, using a microtome (RM2255, Leica, Wetzlar, Germany) for paraffin-embedded tissues and a Reichert cryostat (CM3050S, Leica) for frozen tissues, and were stained with hematoxylin and eosin and periodic acid-Schiff using a standard protocol. The frozen skin tissues were immunostained with rat anti-mouse F4/80 (1:100; kindly provided by the Department of Human Genetics, Leiden University Medical Center, Leiden, The Netherlands), rat anti-mouse CD3 (1:20; Abcam, Cambridge, MA), rat anti-mouse VCAM-1 (1:400; BD Pharmingen, San Diego, CA), rabbit anti-mouse VEGF (1:100; Santa Cruz Biotechnology, Dallas, TX), rabbit anti-VSV (1:2400; Abcam) primary antibodies, followed by anti-rat−IgG-Impress (Vector Laboratories, Burlingame, CA) and anti-rabbit-Envision (Dako, Glostrup, Denmark) horseradish peroxidase-conjugated secondary antibodies with DAB+ as the chromogen. Paraffin-embedded kidney tissues were immunostained with a rabbit anti-human Wilms tumor 1 (1:500; Santa Cruz Biotechnology), followed by anti-rabbit−Envision horseradish peroxidase-conjugated secondary antibody with DAB+ as the chromogen. The frozen kidney tissues were immunostained using rat anti-mouse CD68 (1:15; Abcam), followed by anti-rat−IgG-Impress horseradish peroxidase-conjugated secondary antibody with DAB+ as the chromogen. Double-label immunofluorescence was performed with rat anti−VCAM-1 and goat anti−von Willebrand factor (Affinity Biologicals Inc, Ancaster, Canada), followed by the appropriate secondary antibodies, after which the slides were mounted using Vectashield plus DAPI (Vector Laboratories). For each immunostaining experiment, a nonspecific isotype-matched antibody was used as a negative control.

Digital image analysis and scoring

Images of tissue sections were digitized using a Philips Ultra-Fast Scanner 1.6 RA (Philips Digital Pathology, Best, The Netherlands). For the measurement of epidermal thickness, 10 measurements per field in five randomly selected fields per sample were determined at ×20 magnification using ImageJ software (National Institutes of Health, Bethesda, MD). To determine skin expression of F4/80, VCAM-1, and VEGF, the immunostained surface was measured relative to the total surface area of the skin, in five randomly selected fields per sample at ×20 magnification using ImageJ. Both dermal and epidermal staining of VEGF were measured. CD3-positive cells were counted in five randomly selected fields per sample at ×20 magnification. The surface area of the glomerular tuft, the number of podocytes, and the number of macrophages were quantified as described previously (Bus et al., 2017a).

Cytokine analysis

Sera collected at week 15 post-transfection were quantified for tumor necrosis factor-α and IL-6 by Luminex according to the manufacturer's instructions (Bio-Rad Laboratories, Hercules, CA).

Measurement of the urine albumin-to-creatinine ratio

To measure the urine albumin-to-creatinine ratio, spot urine was collected at 5 and 15 weeks after transfection. Urine albumin levels were measured using rocket immunoelectrophoresis with a rabbit anti-mouse albumin; purified mouse serum albumin (Sigma-Aldrich, Saint Louis, MO) was used as a standard. Urine creatinine was measured using a creatinine assay, with picric acid, sodium hydroxide, and creatinine standards (Sigma-Aldrich); the albumin-to-creatinine ratio was then calculated.

Statistics

For comparison of groups, we used one-way analysis of variance, thereby

taking into account possible differences in variances among groups, based on the Levene's test. Where appropriate, one-way analysis of variance was tested using a log scale. Differences were considered significant at $P < 0.05$.

SUPPLEMENTAL REFERENCES

Bus P, Pierneef L, Bor R, Wolterbeek R, van Es LA, Rensen PC, et al. Apolipoprotein C-I plays a role in the pathogenesis of glomerulosclerosis. J Pathol 2017a;241:589–99.

Bus P, Scharpfenecker M, Van Der Wilk P, Wolterbeek R, Bruijn JA, Baelde HJ. The VEGF-A inhibitor sFLT-1 improves renal function by reducing endothelial activation and inflammation in a mouse model of type 1 diabetes. Diabetologia 2017b;60:1813–21.

Eefting D, Grimbergen JM, de Vries MR, van Weel V, Kaijzel EL, Que I, et al. Prolonged in vivo gene silencing by electroporation-mediated plasmid delivery of small interfering RNA. Hum Gene Ther 2007;18:861–9.

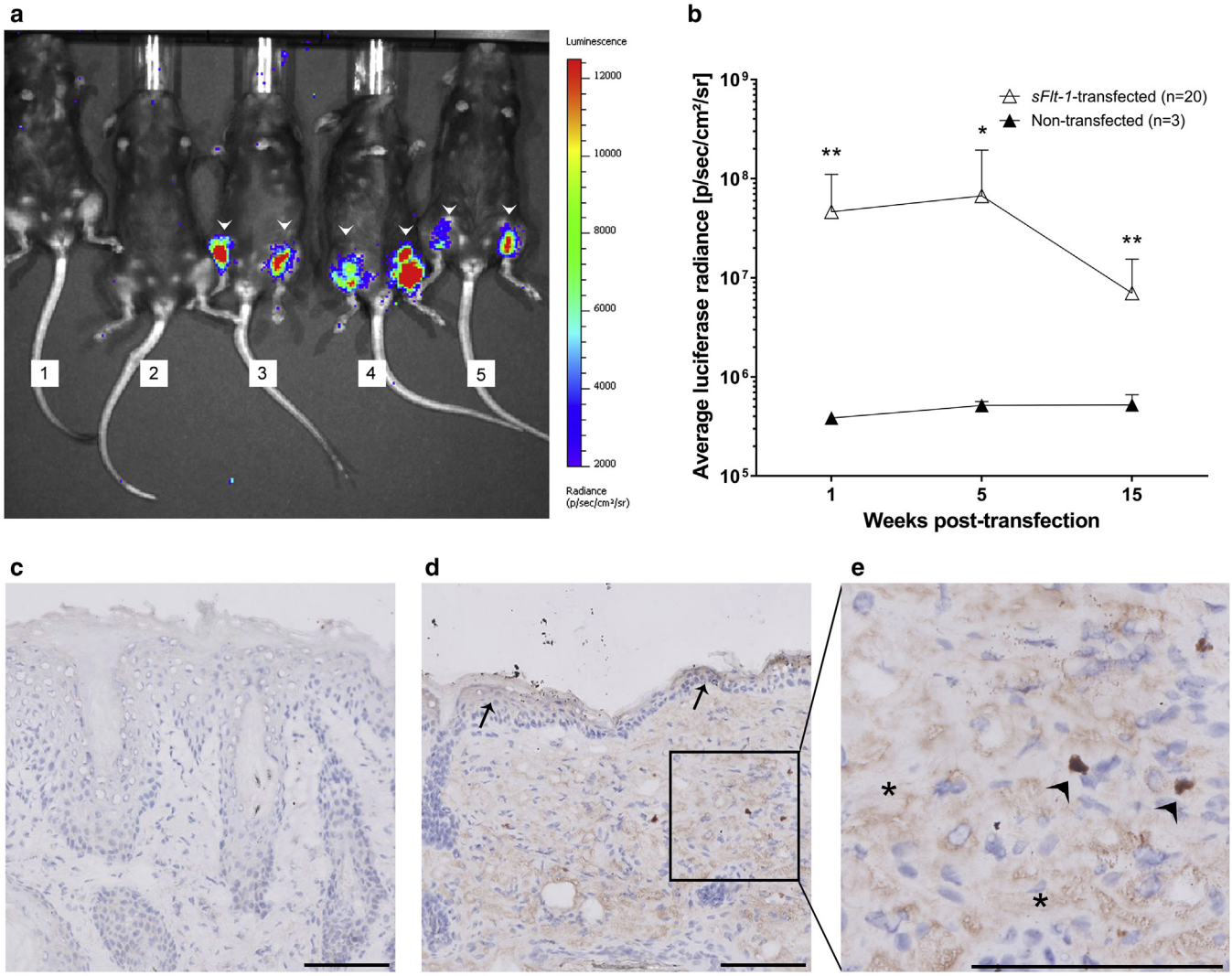

Supplementary Figure S1. Transfection efficiency. The *sFlt-1* and luciferase constructs were co-transfected bilaterally into both gastrocnemius muscles of 8-week-old WT and *APOC1*-tg mice. Following an intraperitoneal injection of luciferin, luminescence was measured and is shown on an (**a**) arbitrary pseudocolor scale; red and blue color correspond to high and low luminescence, respectively. 1 and 2: representative nontransfected *APOC1*-tg mice after an intraperitoneal injection of luciferin; 3–5: representative *sFlt-1*–transfected *APOC1*-tg mice after an intraperitoneal injection of luciferin. No differences in transfection efficiency were observed between WT and *APOC1*-tg mice. (**b**) Quantification of luciferase radiance at 1, 5, and 15 weeks after transfection revealed that the transfected construct was detectable in transfected mice throughout the entire experiment. Representative images of VSV staining in skin sections obtained from a (**c**) nontransfected and a (**d**) transfected *APOC1*-tg mouse at 15 weeks after transfection. Staining for VSV confirmed the presence of the VSV-tagged sFLT-1 protein in the skin of transfected mice. (**d**–**e**) sFLT-1–VSV was present in epithelial (arrows) and stromal skin (asterisks) and in vessels (arrowheads). Summary data are presented as the mean ± standard deviation. $^{*}P < 0.05$ and $^{**}P < 0.01$ versus nontransfected controls. APOC1, apolipoprotein C1; *APOC1*-tg, *APOC1* transgenic; *sFLT-1*, soluble fms-like tyrosine kinase-1; WT, wild-type. Bars = 100 μm.

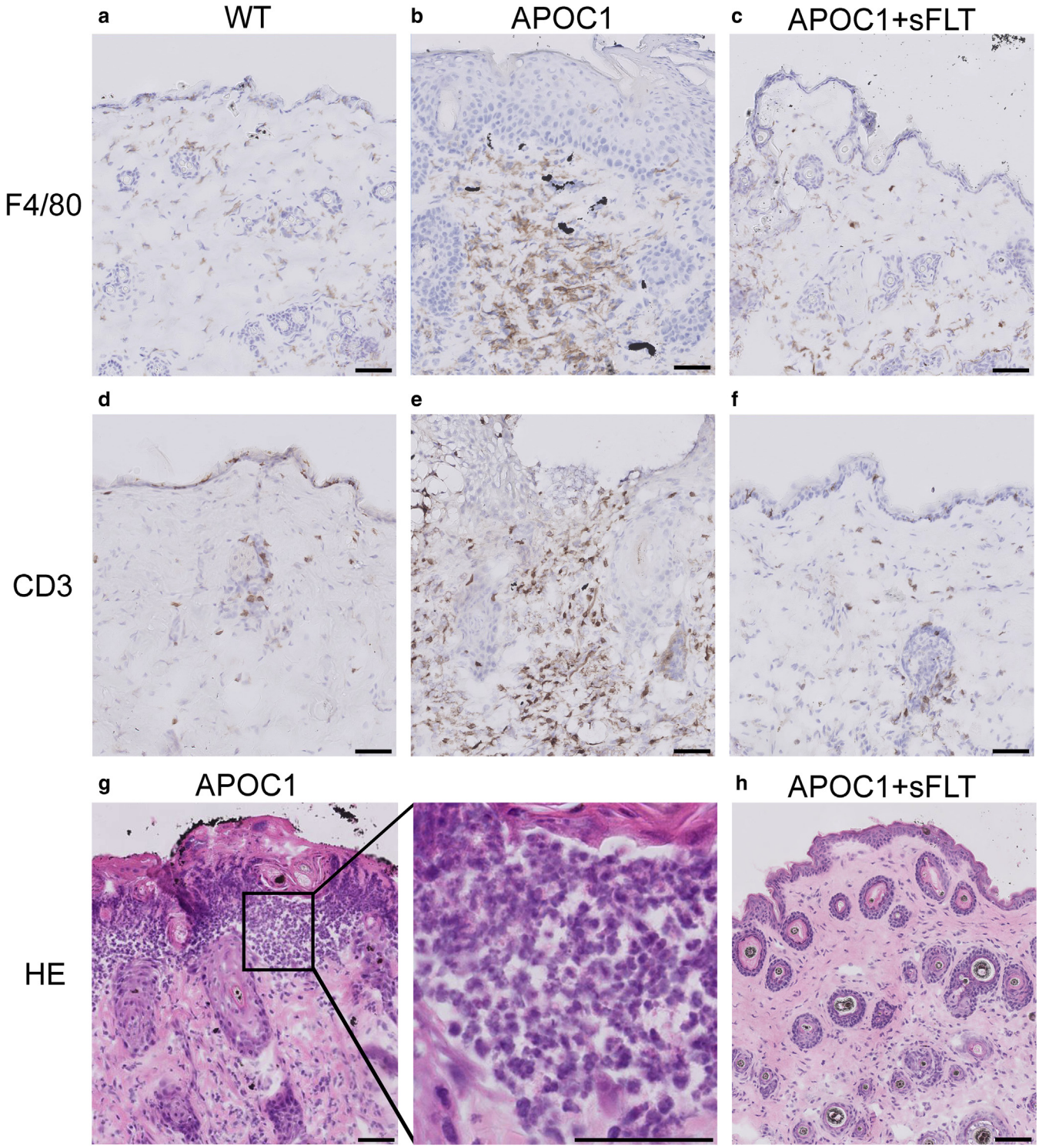

Supplementary Figure S2. Skin expression of F4/80 and CD3 and neutrophils. (**a**–**f**) Representative images of (a–c) F4/80 and (d–f) CD3 staining in skin sections from WT, *APOC1*-tg, and *sFlt-1*–transfected *APOC1*-tg mice at 15 weeks after transfection. (**g, h**) Representative image of (g) an infiltrate containing neutrophils in the skin of a nontransfected *APOC1*-tg mouse, representative image of (h) the skin of a *sFlt-1*–transfected *APOC1*-tg mouse, where neutrophils were not observed; these (g, h) were stained with hematoxylin and eosin. APOC1, apolipoprotein C1; *APOC1*-tg, *APOC1* transgenic; *sFlt-1*, soluble fms-like tyrosine kinase-1; WT, wild-type. Bars = 50 μm.

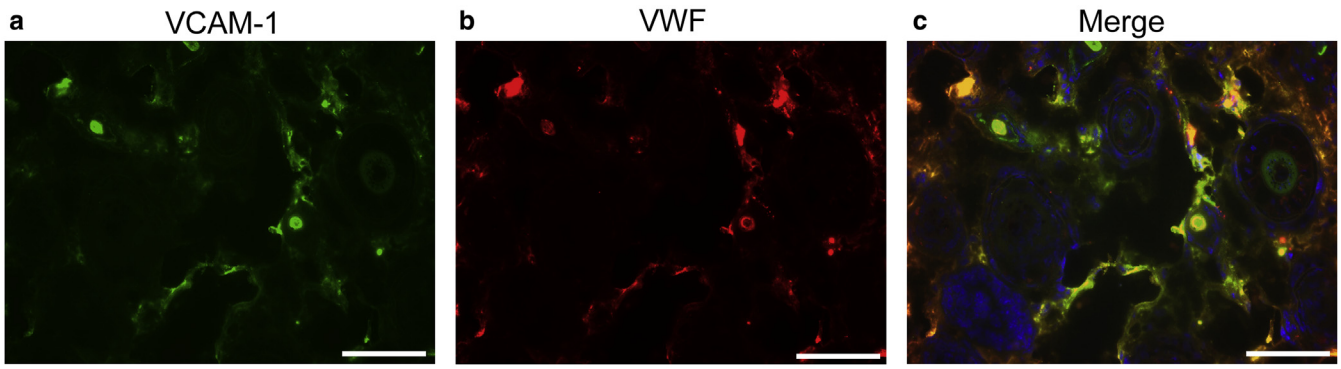

Supplementary Figure S3. Skin VCAM-1 expression in endothelial cells. (**a**–**c**) Double-label immunostaining for (a) VCAM-1 and (b) vWF in the skin of a nontransfected *APOC1*-tg mouse revealed that (c) VCAM-1 colocalizes with vWF, indicating that VCAM-1 is expressed by endothelial cells. *APOC1*-tg, *APOC1* transgenic; vWF, von Willebrand factor. Bars = 50 μm.

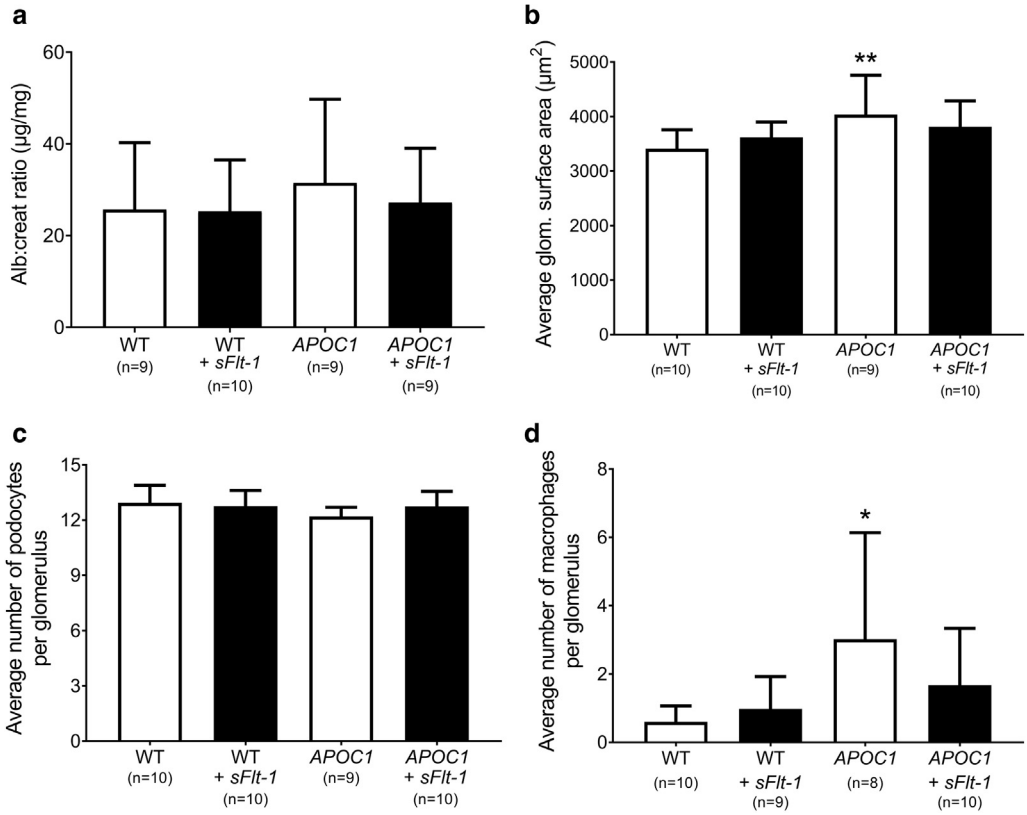

Supplementary Figure S4. Overexpressing *sFlt-1* in WT and *APOC1*-tg mice for 15 weeks does not cause albuminuria or glomerular changes. (**a**–**d**) Fifteen weeks after transfection with *sFlt-1*, (a) the albumin-to-creatinine ratio, (b) glomerular surface area, (c) number of podocytes, and (d) macrophages per glomerulus were measured. Summary data are presented as the mean ± standard deviation. $*P < 0.05$ and $**P < 0.01$ versus nontransfected WT (one-way analysis of variance). APOC1, apolipoprotein C1; *APOC1*-tg, *APOC1* transgenic; *sFlt-1*, soluble fms-like tyrosine kinase-1; WT, wild-type.